Desalination and Water Treatment
www.deswater.com

doi: 10.5004/dwt.2018.22152

109 (2018) 17–27
March

Draw channel contraction of an 8040 spiral-wound forward osmosis membrane element in pressure-assisted forward osmosis (PAFO)

Muhammad Alvan Hidayat[a], Seungho Kook[a], In S. Kim[a,b,*]

[a]*School of Earth Sciences and Environmental Engineering, Gwangju Institute of Science and Technology (GIST), 123 Cheomdangwagi-ro, Buk-gu, Gwangju 61005, Korea, email: iskim@gist.ac.kr (I.S. Kim)*
[b]*Global Desalination Research Center, Gwangju Institute of Science and Technology (GIST), 123 Cheomdangwagi-ro, Buk-gu, Gwangju 61005, Korea*

Received 3 January 2018; Accepted 20 February 2018

ABSTRACT

Pressure-assisted forward osmosis (PAFO) operations were conducted using a pilot system under additional hydraulic pressures ranging from 0 to 4 bar (applied to the feed side) in order to evaluate the effect of feed hydraulic pressure of an 8040 spiral-wound forward osmosis membrane element. The changes in water flux, dilution ratio and pressure build-up in draw stream are mainly observed. The results show a water flux up to 78 L/m^2/h (LMH) compared with conventional forward osmosis along with a higher dilution ratio of around 72.5% in the draw stream. This study also identified a drawback of the usage of spiral-wound membrane element on PAFO configuration due to the pressure build-up in the draw stream that reaches up to 4.4 bar which is caused by draw channel contraction when additional feed hydraulic pressure is applied. The pressure build-up also resulted in a higher energy consumption under higher additional pressure because of the need of additional energy input for the draw channel to be maintained in its original dimensions. The cause of the pressure drop is also observed in this study by analyzing the friction factors.

Keywords: Pressure-assisted forward osmosis (PAFO); Spiral-wound FO; Draw channel contraction; Pressure loss; Energy consumption

1. Introduction

Forward osmosis (FO) as an emerging membrane technology has gained much attention for the past decades and there have been many improvements in the academic world and in the industrial field. It has been suggested as a novel desalination technology to replace existing seawater reverse osmosis (SWRO) process [1–4]. The implementation of FO process also has been tested for wastewater treatment and relevant studies have been increasing steadily in treating synthetic domestic wastewater and municipal wastewater effluents [5–9].

FO is a natural phenomenon which utilizes osmotic pressure as the main driving force. It draws the water molecules from the feed stream across the semipermeable membrane to the draw stream of a higher concentration. Since the driving force is naturally created due to the osmotic pressure difference, FO gives advantages over hydraulic pressure–driven membrane technology such as lower fouling propensity and lower energy consumption [10–12].

With its beneficial usage and potential application, FO is still facing many challenges due to its limitations. The first limitation that prevents application of FO as an independent process or a stand-alone system is the phenomenon of concentration polarization (CP) which reduces the osmotic pressure difference across the membrane causing a lower water productivity [13]. The second limitation is developing a suitable draw solution that can generate high osmotic pressure to produce high water flux for water production and its reconcentration and recovery. Currently, the separation

* Corresponding author.

Presented at the 10th International Desalination Workshop (IDW 2017), November 22–25, 2017, Busan, Korea.

and recovery of the draw solution requires an additional process which resulted in additional energy consumption, therefore still remains a significant challenge for water production especially for drinking water applications. It is urgently needed to find the appropriate draw solutions and a breakthrough on molecular design for a high performance FO membrane [14,15].

Pressure-assisted forward osmosis (PAFO) is considered a promising alternative to overcome the limitations of FO. In PAFO, hydraulic pressure on the feed side acts as additional driving force for water transport along with the osmotic pressure, resulting in enhanced water flux and reduced reverse salt flux. PAFO mainly aims to improve the water permeation by pressurizing the feed and overall efficiency of the system, thereby potentially reducing capital expenditure of the FO process [13,16].

In previous studies, fouling was found to be a problem due to the additional hydraulic pressure in PAFO which leads to severer fouling and compacted cake layer formed compared with FO. However, the suggested osmotic backwashing with subsequent water flushing was proven to be effective to clean the membrane [16,17]. Another study also verified this phenomena showing that the water flux increased linearly with the increase of additional feed hydraulic pressure and lower reverse solute flux due to the water transport originated from the additional feed hydraulic pressure [13]. This shows clear potential of PAFO in engineered osmosis process applications.

Studies on FO processes have been conducted in lab-scale utilizing FO flat sheet membrane coupon and also in pilot-scale utilizing FO spiral-wound modules [18–21]. On the other hand, studies on PAFO have been limited in lab-scale tests and there is not many publications regarding PAFO performance analysis application on a pilot test scale [22–24]. Apparently data produced by lab-scale cannot be directly applied on a large-scale application due to differences in terms of configuration and flow path distances between flat sheet coupons and spiral-wound membrane elements [24,25]. Therefore, PAFO studies in pilot-scale is urgently needed to foresee the potential of PAFO process on a large scale especially on the improvement of the interaction between mass transport produced and water flux. These two factors are very much affected by characterization and design of the spacers within the feed and draw channel spacers based on angles, mesh size, thickness, strand size and void space. The flow path and direction due to the characteristic of the spacer will affect the friction factor within the channel. Until now, little was known about these phenomena on FO and PAFO [26].

Hybrid desalination of two or more water separation processes has been suggested to overcome the drawbacks of the existing desalination technologies. The PAFO–RO hybrid process has been suggested to reduce the energy consumption in desalination plants [27,28]. The PAFO process functions as a pretreatment followed by RO in this scheme by diluting the seawater with impaired water sources and transporting the diluted seawater to the following RO process to lower the energy consumption and improve the overall plant cost effectiveness.

This study aims two specific objectives: (1) observation on the effects of feed hydraulic pressure on 8040 FO spiral wound membrane element on pilot-scale tests and (2) phenomenological investigation of the occurrence of draw channel contraction due to feed hydraulic pressure considering feed hydraulic pressure with initial feed and draw flowrates as major independent variables without circulating draw streams. The resulting pressure build-up and pressure-drop patterns were analyzed to have a better understanding on the current drawbacks of the FO membrane element. This study is devoted to offer practically applicable findings focusing on energy aspects for practical field applications of PAFO using the 8-inch FO membrane element.

2. Materials and methods

2.1. Spiral-wound FO membrane element and PAFO pilot system

An 8-inch spiral-wound CSM RE8040-FO membrane element (Toray Chemical Korea, Inc., Korea) was employed throughout the tests. The membrane element contains 12 polyamide thin-film composite (PA-TFC) membrane leaves with a total effective membrane area of 15.3 m^2. Under standard test condition specified by the manufacturer, water permeation using this membrane element was 35 LMH using DI water for feed and 1 M NaCl for draw. The flow patterns and the characteristics of the spiral wound membrane are shown in Fig. 1(a). The core tube is divided into two parts to direct the draw solution from the draw inlet through the membrane leaf and with the help of the glue lines, they guided the draw solution to the draw stream outlet. The glue line has a function to attach two layer of membrane leaf together where the draw solution flows in between them.

For this study, a single module FO pilot system was used to conduct each experiment. The system consists of FO membrane module, hydraulic pump, flow meter, conductivity meter, pressure valve and temperature regulator. Fig. 1(b) illustrates the single module PAFO pilot testing system. To minimize the effect of hydraulic pressure within the element on the membrane performance, the pressure difference (ΔP) between the feed outlet and the draw inlet was maintained at 0.21 ± 0.01 bar to ensure stable and safe PAFO operation that such minor pressure on the feed side prevents membrane leaves from rupturing of the glue lines. The desired ΔP was maintained by adjusting the bypass and pressure control valves.

The feed stream was circulated throughout the experiment and the feed tank is constantly drained and refilled to maintain the initial feed concentrations in the feed tank. On the contrary, the draw streams were not circulated and the diluted draw streams were collected in the diluted draw tank to maintain the initial draw concentration. Average water flux ($J_{w,\text{ave}}$, LMH) of the element was computed by incorporating effective membrane area and the flowrates at the inlet and outlet of the draw channel; the flowrates were automatically recorded every minute. The $J_{w,\text{ave}}$ calculated using Eq. (1):

$$J_{w,\text{ave}} = \frac{Q_{D,\text{out}} - Q_{D,\text{in}}}{A_{\text{eff}}} \times 60 \quad (1)$$

$Q_{D,\text{out}}$ in Eq. (1) is the flowrate (L/min) at the draw outlet while $Q_{D,\text{in}}$ is the flowrate (L/min) at the draw inlet and A_{eff} is the effective membrane area (i.e., 15.3 m^2) of the membrane element.

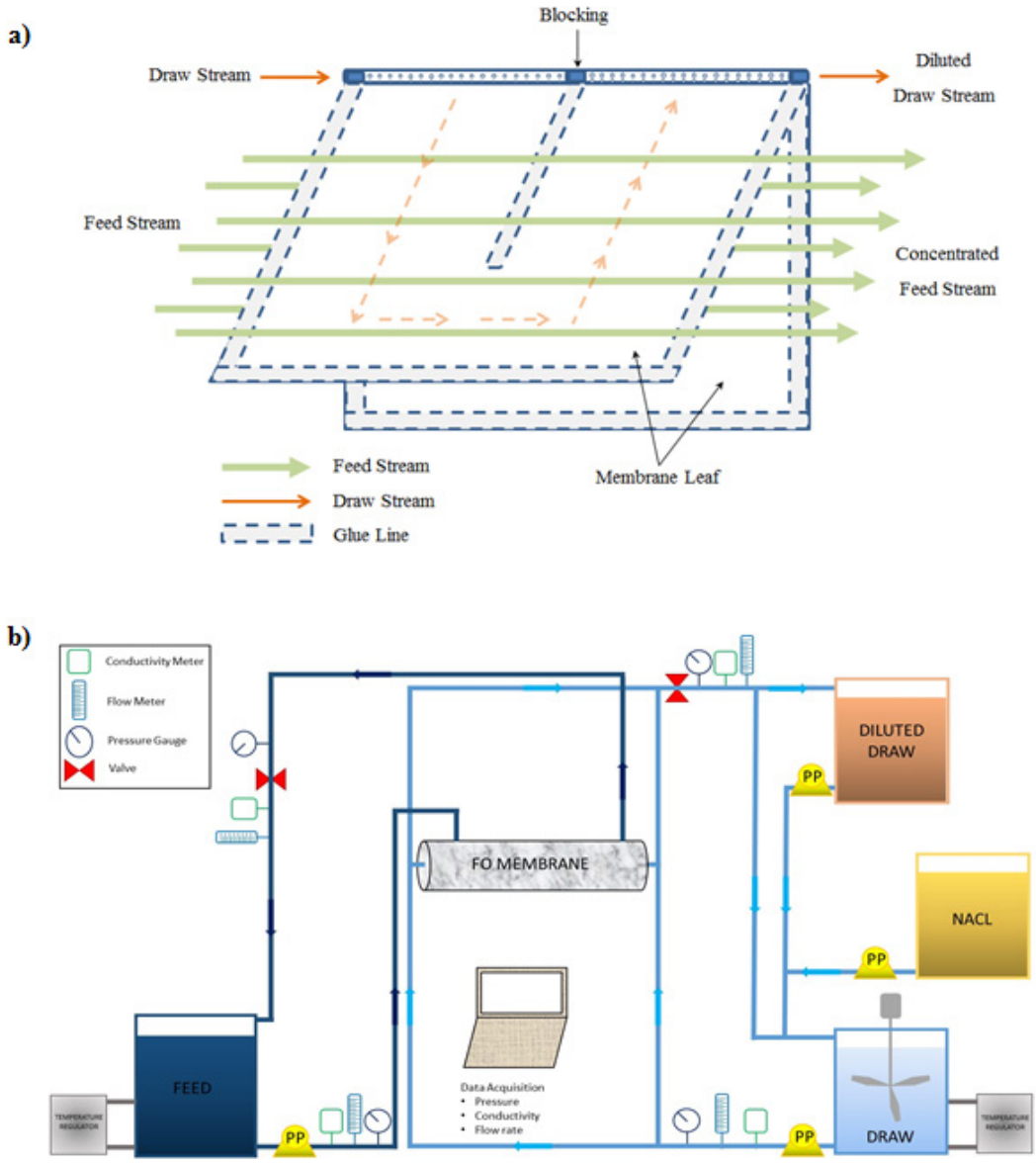

Fig. 1. (a) Flow patterns and characteristics of spiral-wound FO membrane element and (b) schematic of the single module FO pilot testing system.

2.2. Experimental phase

Each set of experiment in this study was separated into three phases as described in Table 1. The first phase was when the pilot system was adjusted on FO mode, meaning pressure difference between feed and draw stream was 0 bar and at the desired feed and draw flowrate condition. The second phase was when only the feed stream controller was adjusted by increasing the feed hydraulic pressure to achieve the desired pressure difference between feed pressure and the draw pressure, meanwhile the draw stream control is untouched. The reason for it was to observe the effect of feed hydraulic pressure increases towards the draw stream condition, the changes within the draw flowrate and draw pressures for instance. The third phase was adjusting both feed and draw stream condition to achieve full PAFO mode, meaning the feed pressure and draw pressure difference was either 1, 2, 3 or 4 bar and at the desired feed and flowrate condition.

Initial feed flowrates (i.e., Q_{F1}) were 50, 60 and 70 L/min and initial draw flowrates (i.e., Q_{D1}) were 5, 6 and 7 L/min. Dilution ratio, DR, was obtained using Eq. (2) to see the degree of dilution compared with the initial draw solution concentration (i.e., seawater concentration = 35 g/L).

$$\mathrm{DR}(\%) = \left(1 - \frac{\text{Diluted draw concentration}}{\text{Seawater concentration}}\right) \times 100 \tag{2}$$

Initial feed solution was tap water with concentration of 200 mg/L to represent the TDS of secondary wastewater effluent and initial draw solution was 35 g/L NaCl (99.5% purity, OCI Company Co., Ltd., Korea) solution. All tests

were conducted at temperature of 25°C ± 1°C for both feed and draw stream. The operating conditions are summarized in Table 2.

3. Results and discussion

3.1. Impact of operating conditions on performance of CSM RE8040-FO membrane element

3.1.1. Average water flux ($J_{w,ave}$)

The flux behavior under different pressure and flowrate was evaluated by operating the system at different feed flowrates: 50, 60 and 70 L/min and different draw flowrates: 5, 6 and 7 L/min. The operating condition was also evaluated based on the pressure difference (ΔP) between the feed outlet and the draw inlet at 1, 2, 3 and 4 bar.

The experiment during FO mode was only able to reach 29.38 LMH of averaged water flux, $J_{w,ave,}$ under the highest feed flowrate and draw flowrate which were 70 and 7 L/min, respectively. However, on PAFO mode when additional hydraulic pressure was applied, the water flux increased up to 78.14 LMH which exceed double the $J_{w,ave}$ of the FO mode operation. Such higher $J_{w,ave}$ of PAFO occurs at the highest condition of ΔP feed and draw flowrates (i.e., flowrate and draw flowrate was 70 and 7 L/min with 4 bar additional feed hydraulic pressure).

Fig. 2 indicates that there can be seen a linear increase within $J_{w,ave}$ as additional feed hydraulic pressure was increased. Each time additional feed hydraulic pressure increased from one pressure condition to another, there can be seen an in $J_{w,ave}$ enhancement ranging from 7 up to 15 LMH. These experiments confirmed the influence of additional feed hydraulic pressure on water flux as discussed in previous studies [16,29,30].

It was also observed that the feed flowrates have an effect on the increase in water flux. As feed flowrate increases, the water flux increases as well. In FO theory, the internal concentration polarization takes place in the porous support layer, meanwhile the external concentration polarization (ECP) occurs on the inter-phase between the rejection layer and surrounding solutions. When flowrate increases, the cross-flow velocity associated with shear force imposed on the membrane surface increased which resulted in the mitigation of ECP, thereby leading to improvement of mass transfer coefficient.

Another reason for the increase in feed flowrate is the spacer configuration. A coarse diamond-shaped spacer is placed in the feed channel of the membrane element. The coarse feed spacer helps create the turbulent flow which then improves the shear stress on the membrane surface where it reduces the effect of ECP. Further discussion regarding the effect of draw flowrate is given in the following section in association with the draw stream dilution.

3.1.2. Dilution ratio

Better dilution of draw solution in PAFO process is in direct correspondence with higher $J_{w,ave}$. As shown in Fig. 3, PAFO mode resulted in a lower concentration in the draw

Table 1
Experimental phases

Phase 1	Phase 2	Phase 3
FO mode (ΔP = 0 bar)	Increased feed hydraulic pressure (ΔP = 1,2,3,4 bar)	PAFO mode (ΔP = 1,2,3,4 bar)
Q_{feed} = 50, 60, 70 L/min	Draw system controller unchanged/untouched	Q_{feed} = normalized
Q_{draw} = 5, 6, 7 L/min		Q_{draw} = normalized

Table 2
Operating conditions for PAFO pilot system test

Operational factors		Description	Note
Membrane element		CSM RE8040-FO	Toray Chemical Korea Inc.
Effective membrane area		15.3	m^2
Initial solutions	Feed	Tap water (1,000 L)	200 mg/L
	Draw	0.6 M NaCl (500 L)	35,000 mg/L
	Stock	5 M NaCl (282 L)	
Flowrates	Feed	50, 60, 70	L/min
	Draw	5, 6, 7	L/min
Temperature	Feed	25°C	±1
	Draw	25°C	±1
Pressure		0, 1, 2, 3, 4	bar
Pressure difference, ΔP		±0.1	ΔP = feed outlet pressure – draw inlet pressure
Operation time		30 min	

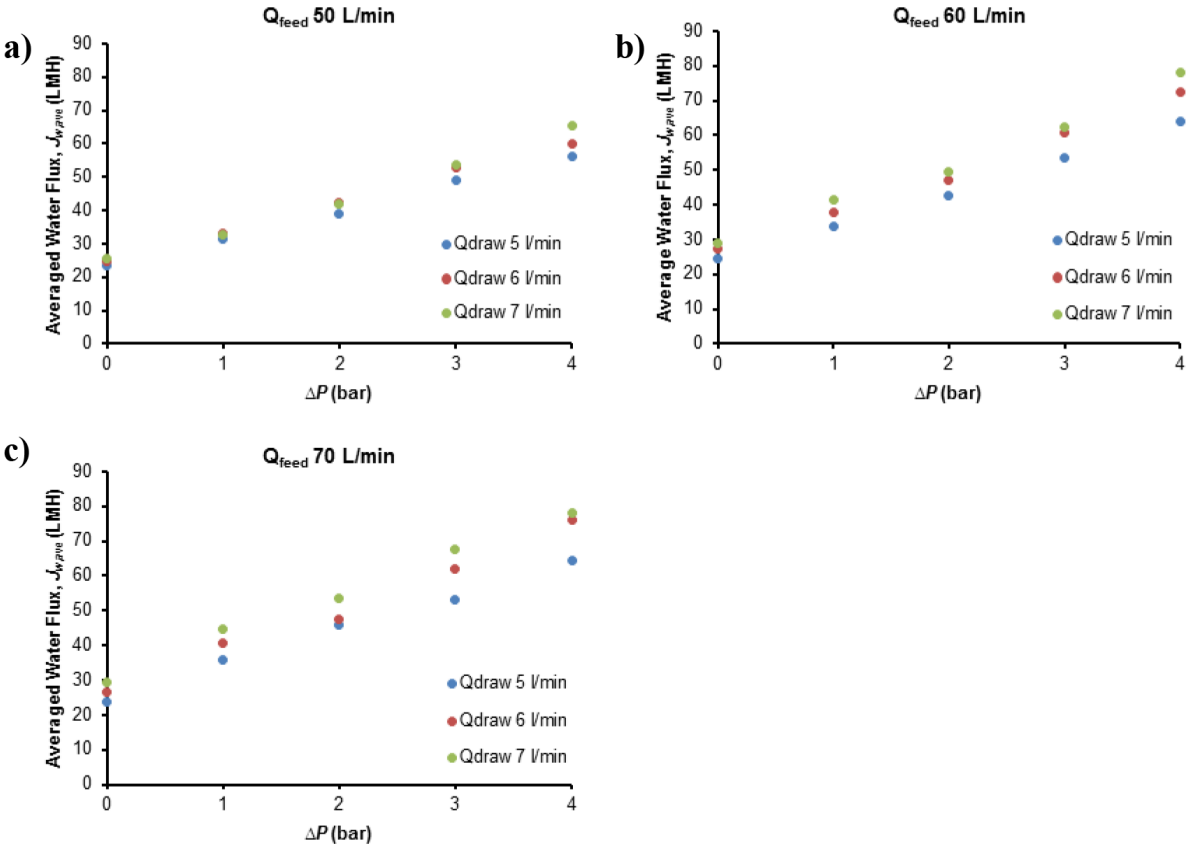

Fig. 2. Averaged water flux under different additional feed hydraulic pressure and varying Q_{draw} when Q_{feed} is (a) 50, (b) 60 and (c) 70 L/min.

stream outlet compared with the FO mode. It also shows that, at a lower draw flowrate, a much higher dilution was achievable compared with the condition of a higher draw flowrate. This is mainly due to, at a lower draw flowrate, the volume of draw stream that was required to be diluted was lower compared with the higher draw flowrate.

During phase 1 (i.e., $\Delta P = 0$ bar), increase of feed flowrate positively affected the draw stream dilution but the increase of draw flowrate had a negative impact. This negative impact was originated from the decrease of retention time of the initial draw body as the draw flowrate increased. On the contrary, during phase 3 (i.e., $\Delta P = 1$–4 bar), this negative impact was mitigated as feed flowrate increased. Compared with FO, which was only able to produce draw stream with a concentration of 16.523 mg/L, PAFO mode was much superior where it was able to produce draw stream with a concentration as low as 9.537 mg/L. This means that FO was only able to achieve around 50% of dilution ratio compared with PAFO which surpasses 70% of dilution ratio.

The capability of PAFO to surpass FO by over 20% in terms of dilution ratio is beneficial in the future prospect of hybrid desalination process such as PAFO–RO hybrid process, since the draw stream product in PAFO will be utilized as the feed stream for RO in the hybrid scheme. The diluted seawater with lower osmotic pressure could reduce the energy consumption that is required to produce a unit volume of product water compared stand-alone SWRO process due to the lower operating pressure [10,28–31].

3.2. Impact of hydraulic pressure on draw channel contraction

3.2.1. Decrease in draw stream flowrate and draw pressure build-up due to draw channel contraction

When increasing the feed hydraulic pressure (i.e., phase shift from phase 1 to phase 2) without controlling the draw side (i.e., draw flowrate and pressure become dependent variables), the draw flowrate was significantly reduced from its initial values. In some condition, it declined to a point where no draw stream outflow was observed.

At a higher initial draw flowrate condition, draw stream was still able to flow through but as the pressure increases the draw flowrate decreased. As shown in Fig. 4 at a condition of feed flowrate of 50 L/min with draw flowrate of 5 L/min under ΔP = 4 bar, the draw stream flowrate was 0 L/min. Similar observations were made when feed flowrates were 60 and 70 L/min, yet to lower degree. Draw channel contraction was mitigated with increasing feed flowrate.

The draw flowrate decline during phase 2 was mainly attributed to the increase of pressure applied on the feed side which caused a contraction of the draw channel which is illustrated in Fig. 5(b). When the operating condition was at phase 1 (FO mode) (i.e., Fig. 5(a)), the system was adjusted to where the pressure on draw stream was enough to flow through the draw channel. However, when the pressure was increased in the feed during phase 2, the draw stream does not have enough pressure to withstand the pressure from the feed which then caused the draw channel to be contracted as the

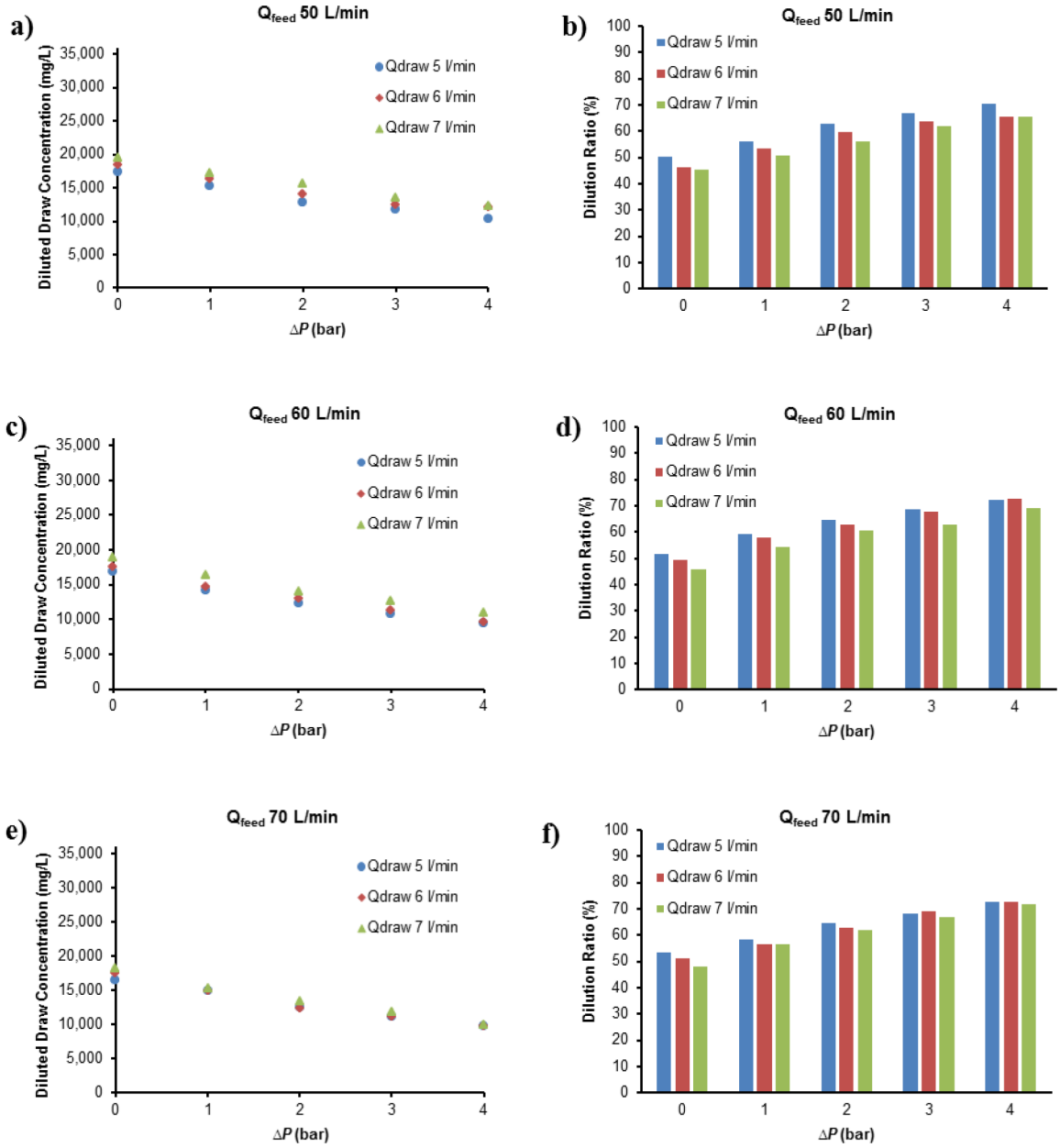

Fig. 3. Diluted draw concentration in the draw outlet (i.e., (a), (c) and (e)) and dilution ratio (i.e., (b), (d) and (f)) when Q_{feed} is 50, (b) 60 and (c) 70 L/min.

pressure builds up in the draw inlet. Also, more significant draw flowrate decline occurred at lower initial draw flowrate when Q_{feed} was 50 L/min. The reason is, when applying low draw flowrate, it requires lower amount of pressure for the draw stream to pass through. Thus, when the draw channel contracted, the draw stream was not able to withstand the pressure from the feed and was not able to flow through the membrane leaf. Therefore, the membrane element lost its capability to flow the initial draw flowrate. Nevertheless, such effect can be reduced by increasing initial feed flowrate.

Flowrate conditions have a significant impact on the pressure. During phase 3, with the increase of desired flowrate condition, either on the feed side or draw side, the pressure that is required to achieve the desired flowrate increases accordingly.

Pressure build-up in the draw inlet is presented in Fig. 6. It explains the amount of increase in term of pressure that occurs in the draw inlet due to the increase of hydraulic pressure difference (ΔP) between the feed and the draw channel under variation of feed and draw flowrate.

With the increase of hydraulic pressure and flowrate, the pressure linearly increased. Pressure build-up increased within the ranges from 0.5 up to 4.14 bar in the draw inlet. It was assumed that the spacer configuration within the draw stream also affects the draw channel contraction. The draw channel is occupied by one coarse spacer (average thickness of 600 μm) and two fine spacers (average thickness of 210 μm) enveloping the coarse spacer.

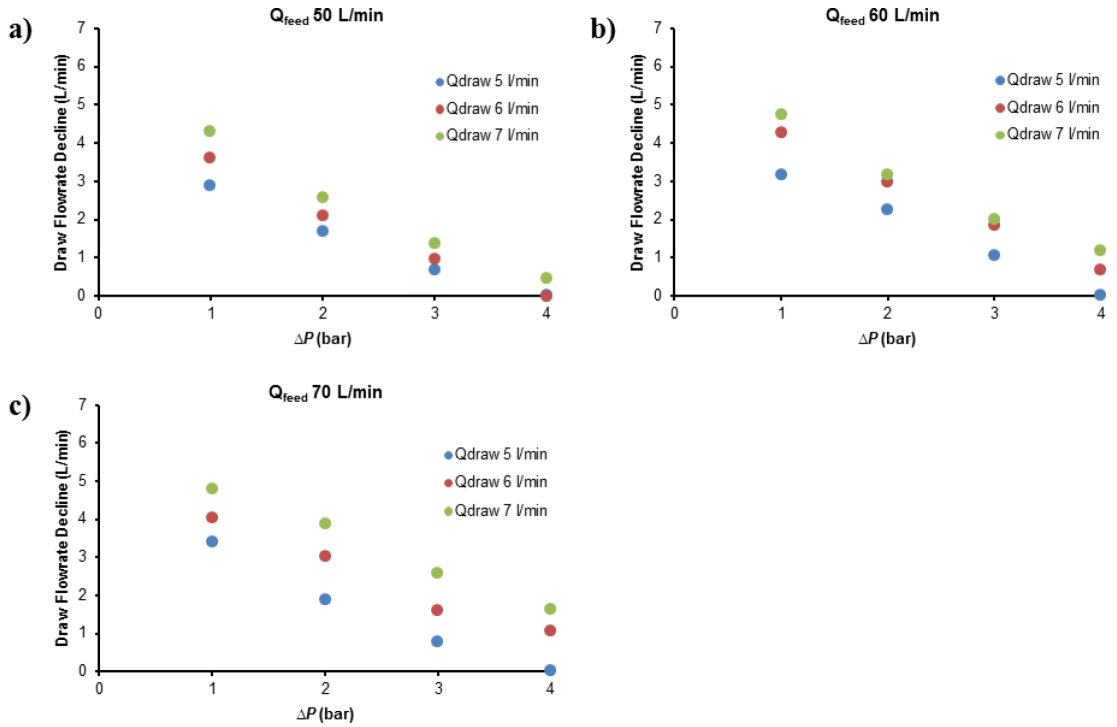

Fig. 4. Draw flowrate decline with applied feed hydraulic pressure at Q_{feed} of (a) 50, (b) 60 (c) 70 L/min.

When adjusting from phase 2 to phase 3, due to the draw channel contraction, the pressure in the draw inlet significantly increased to comply with the capability of withstanding the pressure from the feed and accommodating the initial draw flowrates. During phase 3 (i.e., after the decline of draw flowrate that occurs in phase 2), when increasing the draw flowrate to the initial condition, the draw inlet pressure increased as illustrated in Fig. 5(c). This becomes a burden for the membrane element, because there is an increase of pressure in the draw stream, the feed pressure needed to be adjusted and increased to reach the desired pressure difference during PAFO. Thus, it will have an effect on the life-span of the element and the energy requirement. This will be further elaborated in the following sections.

3.2.2. *Pressure drop associated with friction factor*

Throughout the experiments, we observed significant pressure drops in the draw channel. With the increase of pressure build-up, it affected the amount of pressure drops that occurs. The summary of draw pressure drop is presented in Fig. 7. The pressure drop developed severely in the draw channel compared with the pressure drop that occurs in the feed stream. In the feed stream the pressure drops ranges only from 0.02 up to 0.06 bar. Meanwhile, the pressure drop within the draw stream ranges from 0.81 bar which was at the lowest experimental condition in the experiment (Q_{feed} 50 L/min, Q_{draw} 5 L/min, ΔP = 1 bar) up to 5.41 bar at its highest experimental condition (Q_{feed} 70 L/min, Q_{draw} 7 L/min, ΔP = 4 bar).

To get a better understanding behind the cause of the pressure drop, we used the Darcy–Weisbach equation which explains the phenomena of headloss or pressure loss due to

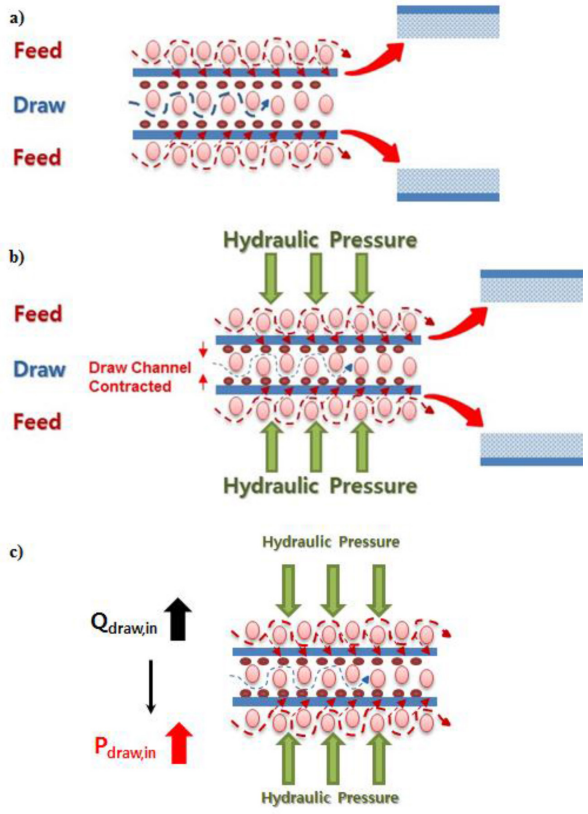

Fig. 5. Illustration of draw channel contraction: the phase shift from (a) phase 1 to (b) phase 2. Draw inlet pressure increase due to pump output adjustment to match the initial draw flowrates depicted in (c).

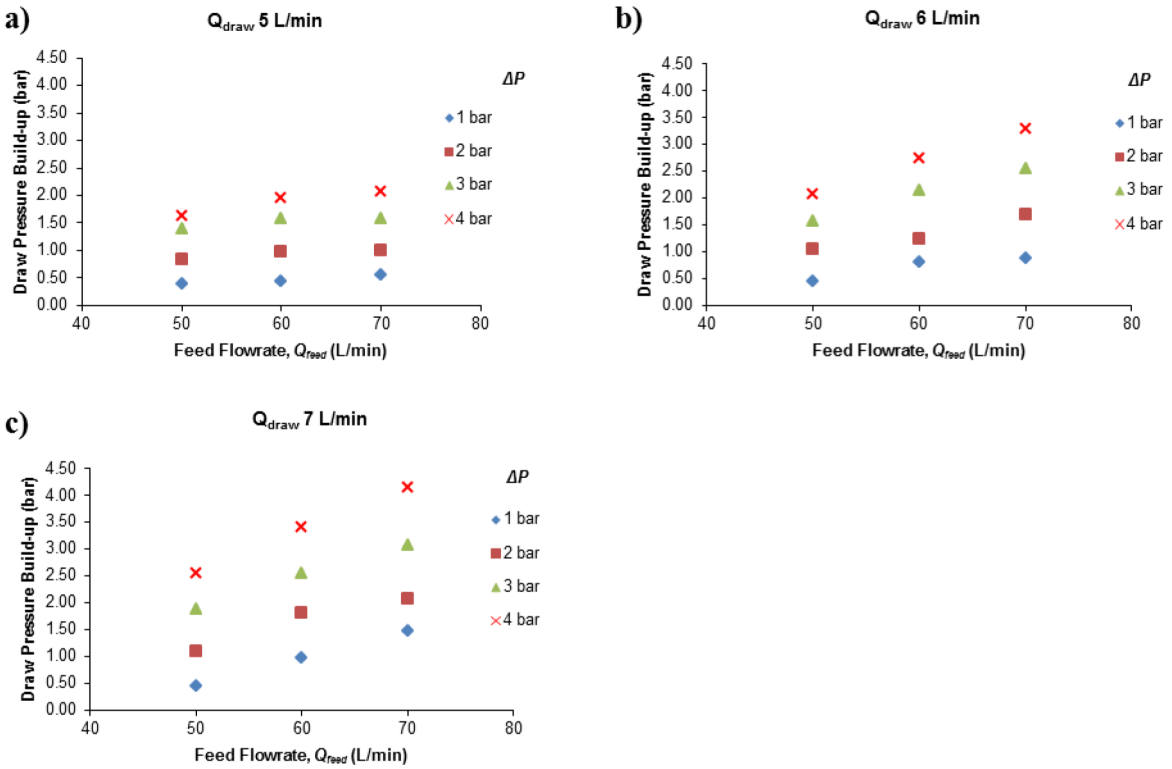

Fig. 6. Pressure build-up in the draw inlet when Q_{draw} is (a) 5, (b) 6 and (c) 7 L/min.

friction. More specifically, we employed the equation to find the Darcy friction factor (f_D) that causes the pressure drop which occurs in the draw channel. Solving the Darcy friction factor can be conducted by modifying Darcy–Weisbach equation shown as follow:

$$f_D = \frac{8gSA^2}{QP} \tag{3}$$

where g is the acceleration due to gravity, A is the cross section area of the draw channel excluding the overall cross section area of the spacers, Q is the flowrate within the draw channel, P is the wetted parameter of the draw channel excluding the overall circumferences of the cross section of the spacers within the draw channel, whereas the head loss per length S can be found by using the following equation:

$$S = \frac{\Delta h}{L} = \frac{1}{\rho g} \cdot \frac{\Delta p}{L} \tag{4}$$

where ϱ is the density of seawater, acceleration gravity g, and length L are known, whereas the pressure loss ΔP (i.e., draw pressure drop) can be found from the experimental results.

The friction factor can be clearly seen to be significantly affected by the experimental conditions and the results are presented in Fig. 7. The results show that the friction factor ranges from 0.13 at the lowest operating condition and up to 0.47 at its highest operating condition. This implies that the experimental conditions have an effect on the friction factors which resulted in increase of pressure drop within the draw channel.

By using Eq. (3), we can observe the other variables that affect the friction factor to cause the pressure drops besides the experimental condition. We can see that the area and wetted parameter of the draw channel plays a role in the increase in friction factor. The area can be found by measuring the channel depth of the draw channel with the length of the draw channel, while the parameter can be found by measuring the wetted parameter of the draw channel. This means that if we could modify the channel depth of the draw stream, it has the potential to lower the friction that occurs in the draw stream which can lower the pressure drop within the draw channel. To modify the channel depth of the draw stream, this could be done by making some modifications in the design and configuration of the draw stream spacers or combinations of draw spacers to guarantee a sufficient draw channel depth for the draw stream to pass through with the minimal friction loss.

3.3. Impact of draw channel contraction on energy consumption

The pressure condition of each operating condition is very much related with energy consumption of the feed and draw pumps. Increases in flowrate and pressure resulted in an increase in pump workload and consequently, energy consumption. When additional feed hydraulic pressure is applied, the draw stream flowrate declined. Therefore, to adjust the draw stream flowrate towards its initial condition, an increase of pressure is required which resulted in an increase on draw pump workload. When there is an increase

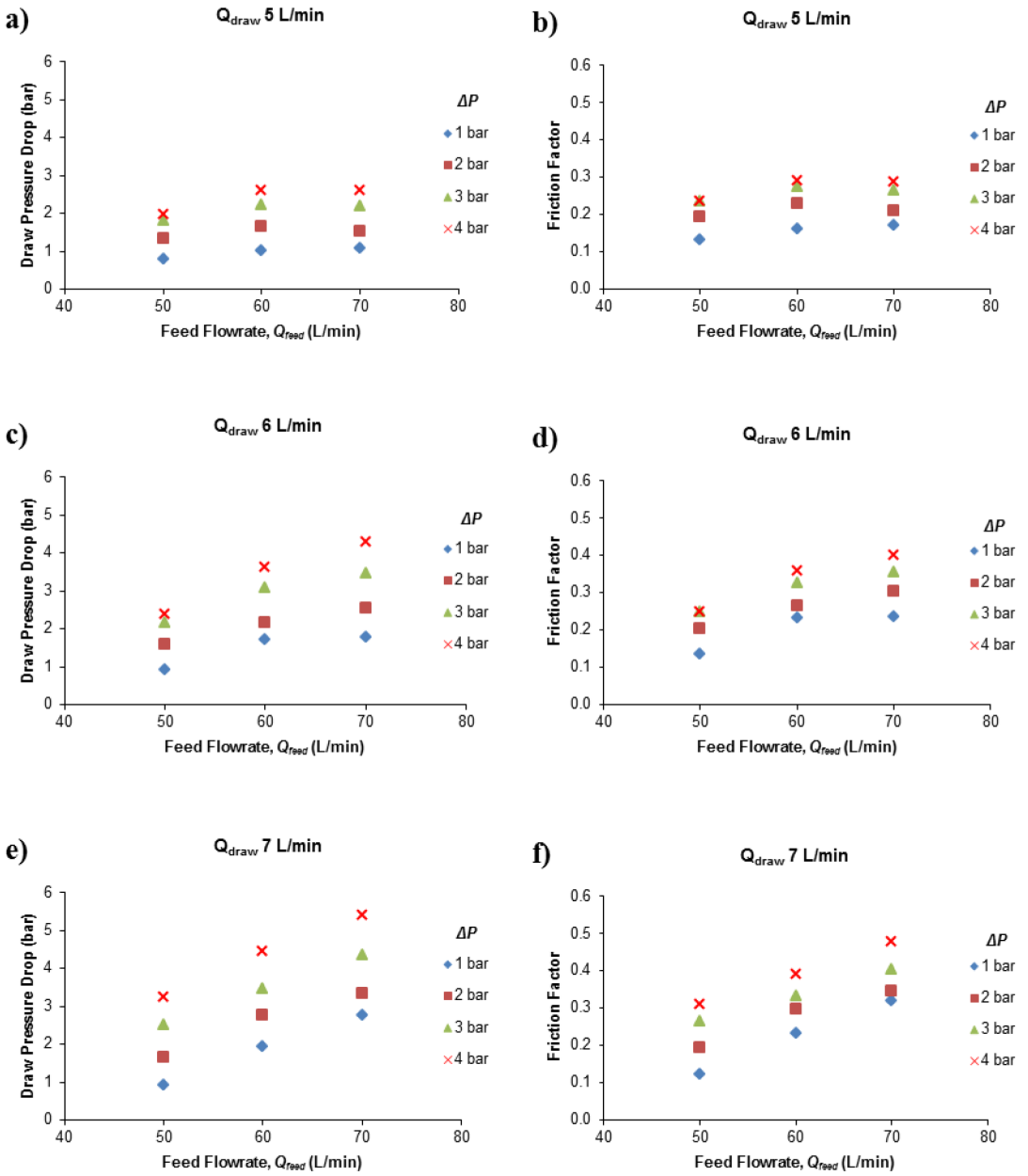

Fig. 7. Pressure drop in the draw channel (i.e., (a), (c) and (e)) and associated friction factors (i.e., (b), (d) and (f)) within the draw channel when Q_{draw} is 5, 6 and 7 L/min.

in draw pressure, feed stream pressure adjustment is also required to achieve the desired pressure condition since it adds additional workload on feed pump.

Energy consumption was obtained by automatic recording by the data acquisition system where it monitors the power of our feed pump. The feed pump has the efficiency of IE3 91.2% while the draw pump has the efficiency of IE3 80.7%. Fig. 8 shows the energy consumption during operating condition of FO mode (phase 1) and PAFO mode (phase 3). The results show the increase in energy consumption even during FO mode as the feed and draw flowrates increase. The recorded energy consumptions were 0.09, 0.105 and 0.135 kWh at feed flowrate of 50, 60 and 70 L/min, respectively. In PAFO mode, when the pressure is much higher than FO mode, it ranges from 0.135 kWh at the lowest flowrate and pressure difference up to 0.750 kWh at the highest flowrate and pressure difference.

4. Conclusions

The impact of feed hydraulic pressure on spiral-wound FO membrane element was discussed in this study, utilizing a spiral-wound 8040 PA-TFC FO element under PAFO condition in pilot-scale. We confirmed the effect of applied feed hydraulic pressure in the improvement of water flux and dilution ratio. However, with the additional hydraulic pressure resulted in a pressure build-up in the draw inlet which becomes a burden for the membrane element and in

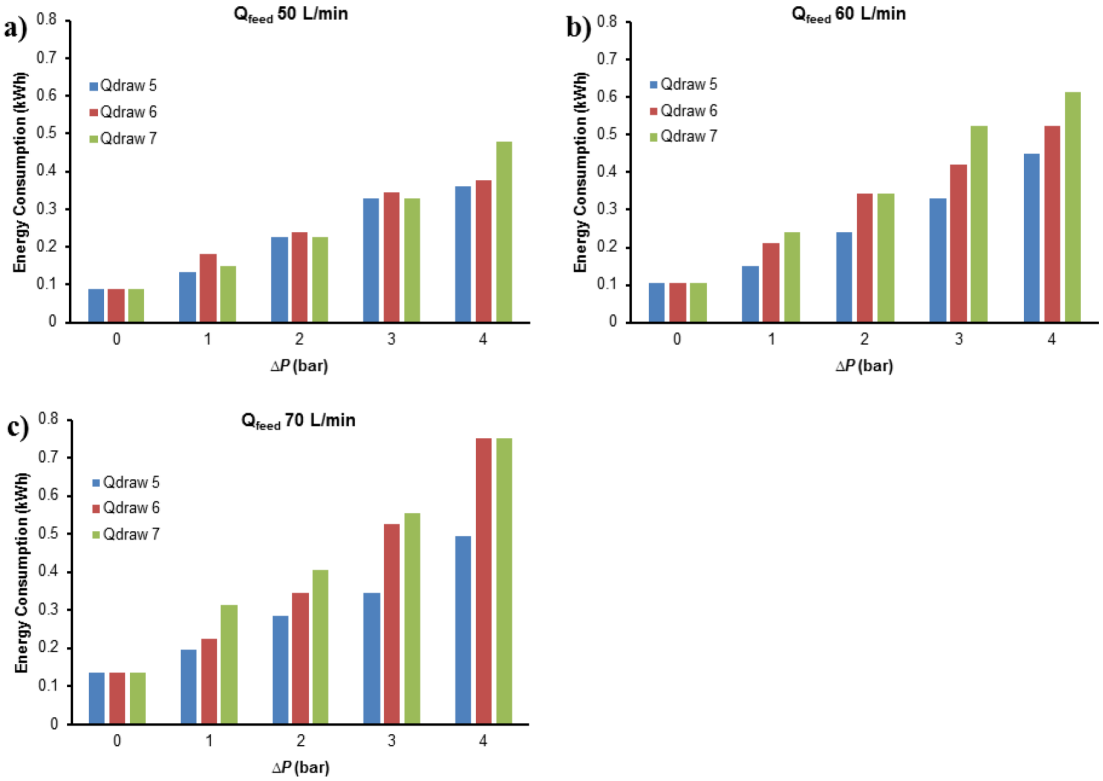

Fig. 8. Summary of energy consumptions when Q_{feed} is (a) 50, (b) 60 and (c) 70 L/min.

the increase of energy requirement for the process. Pressure drops also occurred not only under PAFO condition but also occurred under FO condition. The pressure drop was caused by the friction factor due to the characteristic and design of the spacers which influence the flow pattern and channel depths. This shows that there still are drawbacks within the FO membrane element. Minimizing the pressure dependence of the membrane element, primarily focusing on the draw channel design, is key to improve the feasibility of PAFO in practical terms.

In short, this study gave insights on proper accounting of FO spiral-wound membrane element under PAFO condition on a pilot-scale test to foresee the potential and challenges for the PAFO–RO hybrid system in the future.

Acknowledgements

This research was supported by a grant (code 18IFIP-B087389-05) from Industrial Facilities & Infrastructure Research Program funded by Ministry of Land, Infrastructure and Transport of Korean government.

References

[1] T. Cath, A. Childress, M. Elimelech, Forward osmosis: principles, applications, and recent developments, J. Membr. Sci., 281 (2006) 70–87.
[2] S. Zhao, L. Zou, C.Y. Tang, D. Mulcahy, Recent developments in forward osmosis: opportunities and challenges, J. Membr. Sci., 396 (2012) 1–21.
[3] Q. Ge, M. Ling, T.-S. Chung, Draw solutions for forward osmosis processes: developments, challenges, and prospects for the future, J. Membr. Sci., 442 (2013) 225–237.
[4] L. Chekli, S. Phuntsho, H.K. Shon, S. Vigneswaran, J. Kandasamy, A. Chanan, A review of draw solutes in forward osmosis process and their use in modern applications, Desal. Wat. Treat., 43 (2012) 167–184.
[5] K. Lutchmiah, A.R.D. Verliefde, K. Roest, L.C. Rietveld, E.R. Cornelissen, Forward osmosis for application in wastewater treatment: a review, Water Res., 58 (2014) 179–197.
[6] W. Xue, T. Tobino, F. Nakajima, K. Yamamoto, Seawater-driven forward osmosis for enriching nitrogen and phosphorous in treated municipal wastewater: effect of membrane properties and feed solution chemistry, Water Res., 69 (2015) 120–130.
[7] R. Valladares Linares, Z. Li, M. Abu-Ghdaib, C.-H. Wei, G. Amy, J.S. Vrouwenvelder, Water harvesting from municipal wastewater via osmotic gradient: an evaluation of process performance, J. Membr. Sci., 447 (2013) 50–56.
[8] K. Lutchmiah, E.R. Cornelissen, D.J. Harmsen, J.W. Post, K. Lampi, H. Ramaekers, L.C. Rietveld, K. Roest, Water recovery from sewage using forward osmosis, Water Sci. Technol., 64 (2011) 1443–1449.
[9] X. Zhang, Z. Ning, D.K. Wang, J.C. Diniz da Costa, Processing municipal wastewaters by forward osmosis using CTA membrane, J. Membr. Sci., 468 (2014) 269–275.
[10] L. Chekli, S. Phuntsho, J.E. Kim, J. Kim, J.Y. Choi, J.-S. Choi, S. Kim, J.H. Kim, S. Hong, J. Sohn, H.K. Shon, A comprehensive review of hybrid forward osmosis systems: performance, applications and future prospects, J. Membr. Sci., 497 (2016) 430–449.
[11] J.R. McCutcheon, M. Elimelech, Influence of concentrative and dilutive internal concentration polarization on flux behavior in forward osmosis, J. Membr. Sci., 284 (2006) 237–247.
[12] A.J. Ansari, F.I. Hai, W. Guo, H.H. Ngo, W.E. Price, L.D. Nghiem, Selection of forward osmosis draw solutes for subsequent integration with anaerobic treatment to facilitate resource recovery from wastewater, Bioresour. Technol., 191 (2015) 30–36.
[13] Y. Oh, S. Lee, M. Elimelech, S. Lee, S. Hong, Effect of hydraulic pressure and membrane orientation on water flux and reverse solute flux in pressure assisted osmosis, J. Membr. Sci., 465 (2014) 159–166.

[14] H. Luo, Q. Wang, T.C. Zhang, T. Tao, A. Zhou, L. Chen, X. Bie, A review on the recovery methods of draw solutes in forward osmosis, J. Water Process Eng., 4 (2014) 212–223.
[15] R. Valladares Linares, Z. Li, S. Sarp, S.S. Bucs, G. Amy, J.S. Vrouwenvelder, Forward osmosis niches in seawater desalination and wastewater reuse, Water Res., 66 (2014) 122–139.
[16] G. Blandin, A.R.D. Verliefde, C.Y. Tang, A.E. Childress, P. Le-Clech, Validation of assisted forward osmosis (AFO) process: impact of hydraulic pressure, J. Membr. Sci., 447 (2013) 1–11.
[17] G. Blandin, A.R.D. Verliefde, P. Le-Clech, Pressure enhanced fouling and adapted anti-fouling strategy in pressure assisted osmosis (PAO), J. Membr. Sci., 493 (2015) 557–567.
[18] J.E. Kim, G. Blandin, S. Phuntsho, A.R. Verliefde, P. Le-Clech, H.K. Shon, Practical considerations for operability of an 8″ spiral wound forward osmosis module: hydrodynamics, fouling behaviour and cleaning strategy, Desalination, 404 (2017) 249–258.
[19] C. Boo, M. Elimelech, S. Hong, Fouling control in a forward osmosis process integrating seawater desalination and wastewater reclamation, J. Membr. Sci., 444 (2013) 148–156.
[20] B. Mi, M. Elimelech, Organic fouling of forward osmosis membranes: fouling reversibility and cleaning without chemical reagents, J. Membr. Sci., 348 (2010) 337–345.
[21] S. Kook, J. Kim, S.-J. Kim, J. Lee, D. Han, S. Phuntsho, W.-G. Shim, M. Hwang, H.K. Shon, I.S. Kim, Effect of initial feed and draw flowrates on performance of an 8040 spiral-wound forward osmosis membrane element, Desal. Wat. Treat., 72 (2017) 1–12.
[22] J.E. Kim, S. Phuntsho, F. Lotfi, H.K. Shon, Investigation of pilot-scale 8040 FO membrane module under different operating conditions for brackish water desalination, Desal. Wat. Treat., 53 (2015) 2782–2791.
[23] Y.C. Kim, S.-J. Park, Experimental study of a 4040 spiral-wound forward-osmosis membrane module, Environ. Sci. Technol., 45 (2011) 7737–7745.
[24] S.-J. Im, G.-W. Go, S.-H. Lee, G.-H. Park, A. Jang, Performance evaluation of two-stage spiral wound forward osmosis elements at various operation conditions, Desal. Wat. Treat., 57 (2016) 1–12.
[25] N.T. Hancock, P. Xu, M.J. Roby, J.D. Gomez, T.Y. Cath, Towards direct potable reuse with forward osmosis: technical assessment of long-term process performance at the pilot scale, J. Membr. Sci., 445 (2013) 34–46.
[26] A.R. Da Costa, A.G. Fane, D.E. Wiley, Spacer characterization and pressure drop modelling in spacer-filled channels for ultrafiltration, J. Membr. Sci., 87 (1994) 79–98.
[27] G. Amy, N. Ghaffour, Z. Li, L. Francis, R.V. Linares, T. Missimer, S. Lattemann, Membrane-based seawater desalination: present and future prospects, Desalination, 401 (2017) 16–21.
[28] G. Blandin, A.R. Verliefde, J. Comas, I. Rodriguez-Roda, P. Le-Clech, Efficiently combining water reuse and desalination through forward osmosis-reverse osmosis (FO-RO) hybrids: a critical review, Membranes, 6 (2016).
[29] T.G. Yun, Y.J. Kim, S. Lee, S.K. Hong, Pressure assisted forward osmosis: effect of membrane materials and operating conditions, Procedia Eng., 44 (2012) 1906.
[30] G. Blandin, A. Verliefde, P. Le-Clech, Pressure-assisted osmosis (PAO)–RO hybrid: impact of hydraulic pressure on fouling and economics, Desal. Wat. Treat., 55 (2015) 3160–3161.
[31] S. Liyanaarachchi, V. Jegatheesan, S. Muthukumaran, S. Gray, L. Shu, Mass balance for a novel RO/FO hybrid system in seawater desalination, J. Membr. Sci., 501 (2016) 199–208.